

Heavily electron-doped electronic structure and isotropic superconducting gap in $A_x\text{Fe}_2\text{Se}_2$ ($A=\text{K},\text{Cs}$)

Y. Zhang,¹ L. X. Yang,¹ M. Xu,¹ Z. R. Ye,¹ F. Chen,¹ C. He,¹ J. Jiang,¹ B. P. Xie,¹ J. J. Ying,² X. F. Wang,² X. H. Chen,² J. P. Hu,³ and D. L. Feng^{1,*}

¹State Key Laboratory of Surface Physics, Key Laboratory of Micro and Nano Photonic Structures (MOE), and Department of Physics, Fudan University, Shanghai 200433, People's Republic of China

²Hefei National Laboratory for Physical Sciences at Microscale and Department of Physics, University of Science and Technology of China, Hefei, Anhui 230026, Peoples Republic of China

³Department of Physics, Purdue University, West Lafayette, Indiana 47907, USA

The low energy band structure and Fermi surface of the newly discovered superconductor, $A_x\text{Fe}_2\text{Se}_2$ ($A=\text{K},\text{Cs}$), have been studied by angle-resolved photoemission spectroscopy. Compared with iron pnictide superconductors, $A_x\text{Fe}_2\text{Se}_2$ ($A=\text{K},\text{Cs}$) is the most heavily electron-doped with $T_c \sim 30$ K. Only electron pockets are observed with an almost isotropic superconducting gap of ~ 10.3 meV, while there is no hole Fermi surface near the zone center, which indicates the inter-pocket hopping or Fermi surface nesting is not a necessary ingredient for the unconventional superconductivity in iron-based superconductors. Thus, the sign changed s_{\pm} pairing symmetry, a leading candidate proposed for iron-based superconductors, becomes conceptually irrelevant in describing the superconducting state here. A more conventional s-wave pairing is a better description.

PACS numbers: 74.25.Jb, 74.70.-b, 71.18.+y

Since the discovery of iron-based high temperature superconductors in 2008 [1, 2], the pairing mechanism of this new class of materials has been extensively studied [3–9]. Among various aspects that were suggested to be essential for the unconventional superconductivity, the multi-band nature of the electronic structure arguably received the most attention [10]. In particular, in the weak coupling approach, it was suggested that the superconductivity could be boosted by the nesting or hopping between the electron-like Fermi surfaces near the zone corner and the hole-like Fermi surfaces near the zone center [8], and the sign change of the superconducting order parameters between the hole and electron Fermi surfaces stems from the inter-pocket scattering [3]. Moreover, The gap symmetry and gap anisotropy (e.g. the appearance of nodes) are sensitive to the presence of certain Fermi surface and the interactions among the bands [11]. However, in the strong coupling approach, the superconducting pairing is dominated by the intra-orbital pairing and relatively robust against the change of band structures [4]. The dominating pairing symmetry is an A_{1g} s-wave. Experimentally, both nodal and nodeless gap distributions have been reported by different techniques in various systems. Although the scanning tunneling spectroscopy (STS) data on Fe(Se,Te) suggest a nodeless s_{\pm} -wave gap [12], the STS data on FeSe indicate a nodal gap [13]. While photoemission data on $\text{Ba}_{1-x}\text{K}_x\text{Fe}_2\text{As}_2$ and $\text{BaFe}_{2-x}\text{Co}_x\text{As}_2$ fit the s_{\pm} -wave gap function well [7–9], the thermal conductivity measurements suggest gap in heavily hole doped KFe_2As_2 to be a nodal type [14]. A conclusion on the pairing behaviors seems to be still far-fetched for the iron based superconductors.

Recently, a new series of iron-based superconductors, $A_x\text{Fe}_2\text{Se}_2$ ($A=\text{K},\text{Cs}$), has been discovered with relatively high transition temperature of ~ 30 K [15–18]. Judging from their chemical formula, these compounds would be the most heavily electron-doped amongst the iron-based superconductors. More importantly, it provides an opportunity to examine the common aspects of the electronic structure and pairing mechanism in iron-based systems from the most electron-doped end. In this paper, we report the angle resolved photoemission spectroscopy (ARPES) study of $A_x\text{Fe}_2\text{Se}_2$ ($A=\text{K},\text{Cs}$). We found that they are indeed the most heavily electron-doped iron-based superconductor. Only electron pockets are observed, while there is no hole Fermi surface near the zone center. The superconducting gap around the electron pockets is isotropic, and about 10.3 meV, i.e. $\sim 4k_B T_c$ for both compounds. Our result indicates the inter-pocket hopping or Fermi surface nesting is not a necessary ingredient for the unconventional superconductivity in iron-based superconductors. Thus the sign change in s_{\pm} -wave pairing, a promising pairing symmetry candidate suggested earlier, is not a fundamental property of iron-based superconductors. Rather, the isotropic gap structure is better to be considered as a more conventional s-wave.

$\text{A}_{0.8}\text{Fe}_2\text{Se}_2$ ($A=\text{K},\text{Cs}$, nominal composition) single crystals were synthesized by self-flux method as described elsewhere in detail [18], which show flat shiny surfaces with dark black color. Fitting the X-ray diffraction data assuming the $I4/mmm$ symmetry gave $a = 3.8912$ Å, $c = 14.1390$ Å for $\text{K}_{0.8}\text{Fe}_2\text{Se}_2$, and $a = 3.9618$ Å, $c = 15.285$ Å for $\text{Cs}_{0.8}\text{Fe}_2\text{Se}_2$. $\text{K}_{0.8}\text{Fe}_2\text{Se}_2$ shows the onset superconducting transition temperature (T_c) of 31.7 K, and it reaches zero resistivity at 31.2 K; while $\text{Cs}_{0.8}\text{Fe}_2\text{Se}_2$ shows the onset T_c of 30 K with a transition width of 2 K in the resistivity data. The magnetic sus-

*Electronic address: dl Feng@fudan.edu.cn

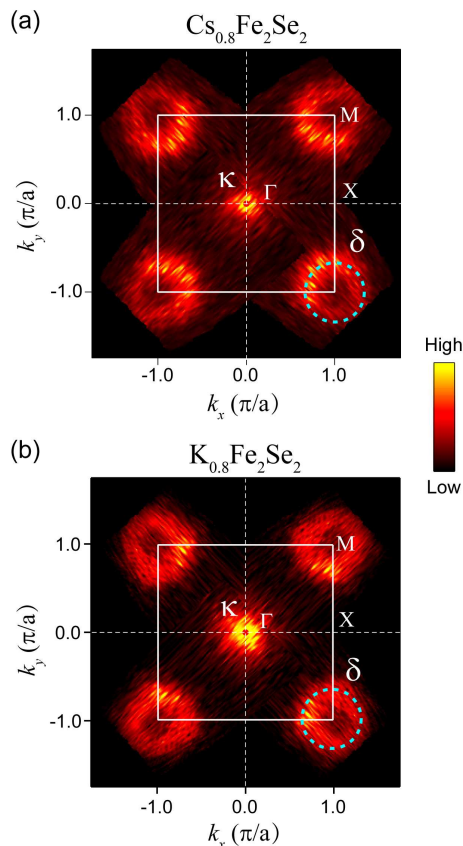


FIG. 1: The four-fold symmetrized photoemission intensity map at the Fermi energy (E_F) for (a) $\text{Cs}_{0.8}\text{Fe}_2\text{Se}_2$, and (b) $\text{K}_{0.8}\text{Fe}_2\text{Se}_2$. The intensity was integrated over a window of $[E_F - 15 \text{ meV}, E_F + 15 \text{ meV}]$.

ceptibility measurements showed almost 100% shielding fraction, indicating the bulk superconducting nature and good quality of the crystals. ARPES measurements were performed with SPECS UVLS discharge lamp (21.2 eV He-I α light) and a Scienta R4000 electron analyzer. The overall energy resolution was set to 9 or 12 meV, and the angular resolution was 0.3° . The sample was cleaved *in situ*, and measured under ultra-high-vacuum of $5 \times 10^{-11} \text{ torr}$. The actual chemical compositions were determined by energy dispersive X-ray (EDX) spectroscopy on the cleaved surface after the photoemission measurements, which gave K : Fe : Se = 0.94 : 1.98 : 2, and Cs : Fe : Se = 0.92 : 1.99 : 2. For simplicity, they are called by the nominal compositions throughout the text.

Figure 1 shows the photoemission intensity maps at the Fermi energy (E_F) for $\text{Cs}_{0.8}\text{Fe}_2\text{Se}_2$ and $\text{K}_{0.8}\text{Fe}_2\text{Se}_2$. The Fermi surface topology is similar in both systems. There is an electron-like Fermi pocket surrounding the zone corner, and some spectral weight is located at the zone center.

The sizes of the electron pocket are about the same for both K and Cs compounds, and their band structures are very much alike as well. Figure 2 further reveals the band structure of $\text{K}_{0.8}\text{Fe}_2\text{Se}_2$. Around the zone center

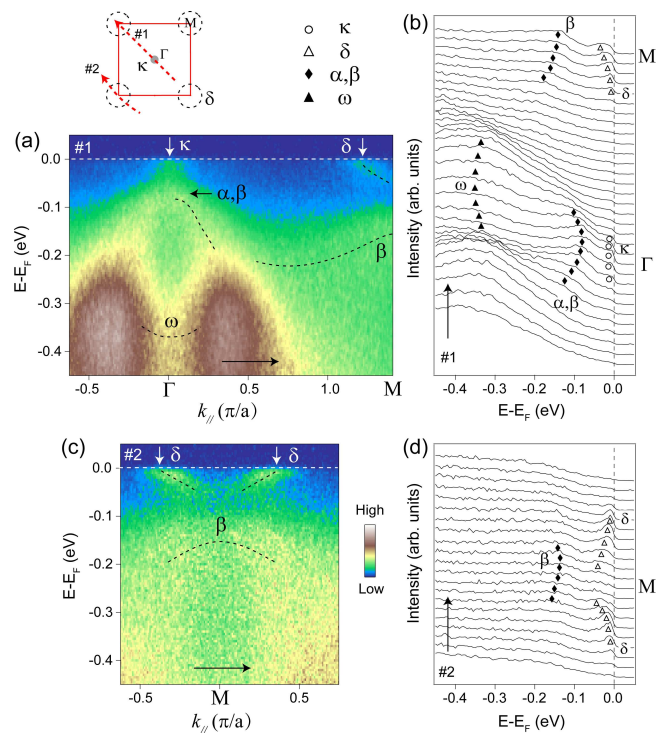


FIG. 2: Photoemission data of $\text{K}_{0.8}\text{Fe}_2\text{Se}_2$. (a) The photoemission intensity, and (b) energy distribution curves (EDC's) along cut #1 or Γ -M in the projected two dimensional Brillouin zone as shown at the top of panel a. (c) and (d) The photoemission intensity, and EDC's along cut #2 across the zone corner respectively.

[Figs. 2(a) and 2(b)], there is a small electron-like feature, the κ band. The spectral weight of this band is rather weak, indicating that it might be a tail of certain band slightly above E_F . This is consistent with a recent band structure calculation that shows an electron pocket in the zone center for $\text{K}_x\text{Fe}_2\text{Se}_2$ at certain doping [19]. At -0.1 eV and below, the fast dispersive features are most likely the α and β bands that form the hole-like pockets in $\text{Fe}(\text{Te},\text{Se})$ [20] and iron pnictides. Moreover, the ω band is observed around 0.35 eV below E_F near Γ , and similar band is observed in iron pnictides and known to be made of the d_{z^2} orbitals [10]. Around the zone corner [Figs. 2(c) and 2(d)], an electron-like band, δ , is observed together with the β band from the zone center. Theoretically, two electron-like bands around M were predicted for $\text{K}_{0.8}\text{Fe}_2\text{Se}_2$ [19], just like for the iron pnictides. However, at certain experimental geometry, only one electron-like band is often observed due to the matrix element of the $3d$ orbitals [10]. It is also predicted that the Fermi crossings of these two bands are almost-degenerate, and the bottom of the other electron like band would coincide with the β band at M [10, 19]. In general, the bands around Γ resemble those observed in $\text{Fe}(\text{Te},\text{Se})$ and iron pnictides, except that the chemical potential is shifted up via electron doping here. Take $\text{BaFe}_{1.85}\text{Co}_{0.15}\text{As}_2$ for a comparison, although it is op-

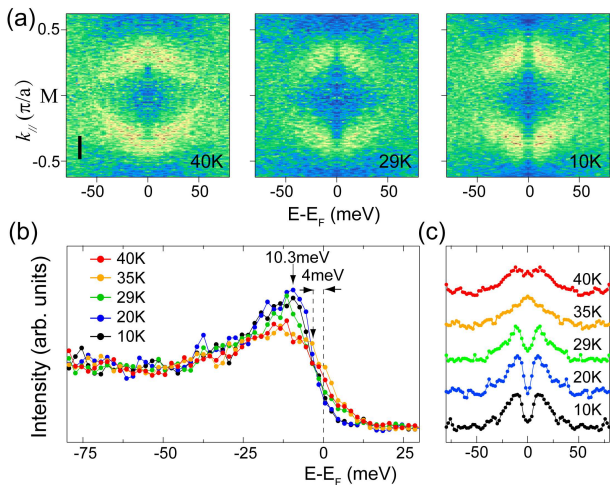


FIG. 3: (a) The symmetrized (with respect to E_F) photoemission intensity of $K_{0.8}Fe_2Se_2$ at 40, 29, and 10 K along the cut #2 in Fig. 2. (b) Temperature dependence of the spectrum integrated over the momentum region indicated by the black bar in panel a, and (c) its stacked symmetrized version. Energy resolution was set to 9 meV in the gap measurements.

timally electron-doped with a T_c of about 25 K, there are still several hole-like pockets around the zone center [10]. Moreover, the binding energy of the ω band near Γ is about 200 meV larger in $K_{0.8}Fe_2Se_2$ than that in $BaFe_{1.85}Co_{0.15}As_2$ due to the higher electron doping in the former compound. However, it is interesting to note that the δ band around M is rather flat and shallow in $K_{0.8}Fe_2Se_2$, indicative of a non-rigid band behavior.

Assuming the electronic structure of $A_{0.8}Fe_2Se_2$ to be two dimensional and two almost-degenerate electron pockets around M, in the ionic picture, we could obtain $3d^{6.18}$ per Fe ion for $A_{0.8}Fe_2Se_2$ by the measured Fermi surface volume. This cannot account for all the electrons in the $3d^{6.45}$ configuration calculated directly from their actual chemical compositions. Therefore, the inconsistency may suggest possible k_z dispersions of the δ and κ bands. To fully reveal the Fermi surface topology, more detailed k_z and polarization dependence studies are required with variable photon energies at a synchrotron facility. In any case, the measured electronic structure clearly shows that $A_{0.8}Fe_2Se_2$ is indeed the most heavily electron-doped iron-based superconductor by far.

To study the superconducting gap of $K_{0.8}Fe_2Se_2$, high resolution data taken above and below T_c along the cut #2 are compared in Fig. 3. As shown in Fig. 3(a), there is no gap at E_F near the Fermi momentum in the normal state, while a clear gap shows up at low temperatures in the superconducting state. The temperature dependence of the spectrum illustrates that the spectral weight near the Fermi energy is depleted and a coherent peak feature grows with decreasing temperature [Fig. 3(b)]. One can clearly identify a leading edge gap of 4 meV at 10 K. Taking the coherent peak position as the superconducting gap, we find it to be ~ 10.3 meV,

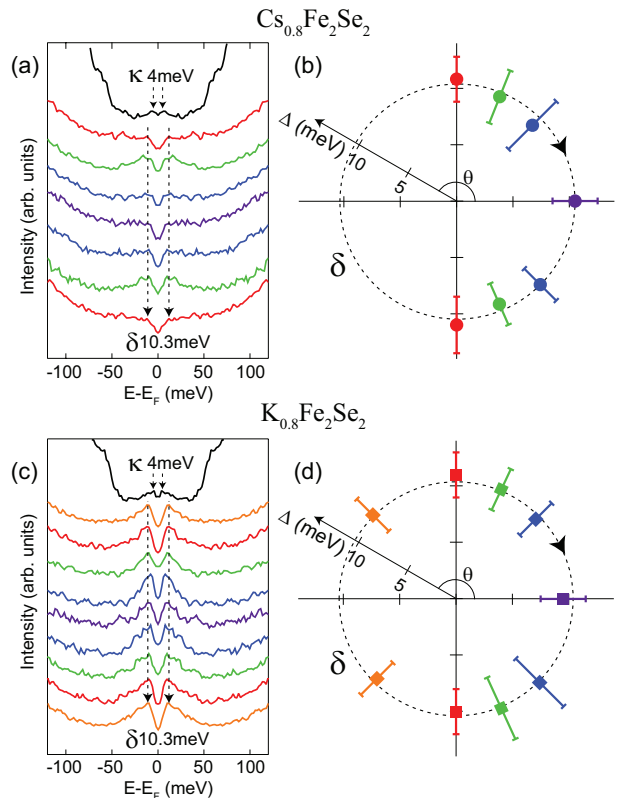


FIG. 4: (a) The symmetrized (with respect to E_F) EDC's at various Fermi crossings for $Cs_{0.8}Fe_2Se_2$. The top curve is for the κ band at Γ , and the rest are for the δ band with momenta clockwise along the δ pocket as shown by the arrows in panel b. (b) Gap distribution of the δ band around M in a polar coordinate, where the radius represents the gap, and the polar angle θ represents the position on the δ pocket with respect to M, with $\theta = 0$ being the M- Γ direction. (c) and (d) are the same as panels a and b except for $K_{0.8}Fe_2Se_2$. All data were taken at 9K.

i.e. $\sim 4k_B T_c$. This ratio between gap and T_c falls into the same regime as other iron-based superconductors [7–9]. The symmetrized spectra in Fig. 3(c) further indicate that the gap disappears when the temperature is above T_c . We note that the spectra are integrated over a small region around the normal state Fermi momentum to compensate the relatively weak signal, but the estimated gap amplitude would not be affected much, as the gap feature in this region is rather flat [Fig. 3(a)].

By examining the symmetrized EDC's in the superconducting state at various Fermi crossings of both the κ and δ bands, the momentum distribution of superconducting gap is deduced in Fig. 4. For both K and Cs compounds, the gap of the δ band around the M point is of the isotropic s-wave type within the experimental uncertainty, which averagely is about 10.3 meV; while the gap is 4 meV for the κ band at Γ . The smaller gap at Γ than those around M certainly violates the simple gap function of $\cos k_x \cos k_y$ for s_{\pm} -wave order parameter, and indicates the gaps may be orbital dependent. More-

over, since the spectral weight near the zone center is minimal, its contribution to the superconductivity would be rather negligible with such a small gap. Therefore, the inter-pocket scattering previously suggested can not be the essential force driving the superconductivity.

In summary, our data show that the rather robust superconductivity in such a highly electron-doped iron-based superconductor could mainly rely on the electron Fermi surfaces near M. The rather unique electronic structure in $A_{0.8}Fe_2Se_2$ ($A=K, Cs$) further highlights the diversity of the iron-based superconductors, and suggests that the superconductivity is very robust against the change of Fermi surfaces. Our data also strongly suggest that the inter-band hopping might not be so sub-

stantial as previous data suggested. Thus, the promising candidate, the so called s_{\pm} wave characterized by the sign change of the superconducting orders between electron and hole pockets, is not a proper description of the superconducting state in $A_xFe_2Se_2$. Instead, the more conventional s-wave type is a more proper and general description for the iron-based superconductors. Our result can also be viewed as a support to the picture derived from the strong coupling approach suggesting the pairing being the intra-orbital pairing caused by local electron-electron correlation.

This work was supported by the NSFC, MOE, STCSM, and National Basic Research Program of China (973 Program) under the grant No. 2011CB921802.

-
- [1] Y. Kamihara, T. Watanabe, M. Hirano, and H. Hosono, *J. Am. Chem. Soc.* **130**, 3296 (2008).
- [2] X. H. Chen, T. Wu, G. Wu, R. H. Liu, H. Chen, and D. F. Fang, *Nature (London)* **453**, 761 (2008).
- [3] I. I. Mazin, *et al*, *Phys. Rev. Lett.* **101**, 057003 (2008).
- [4] K. Seo, B. A. Bernevig, and J. Hu, *Phys. Rev. Lett.* **101**, 206404 (2008).
- [5] F. Wang *et al.*, *Phys. Rev. Lett.* **102**, 1047005 (2009).
- [6] K. Kuroki, S. Onari, R. Arita, H. Usui, Y. Tanaka, H. Kontani, and H. Aoki, *Phys. Rev. Lett.* **101**, 087004 (2008).
- [7] H. Ding, P. Richard, K. Nakayama, K. Sugawara, T. Arakane, Y. Sekiba, A. Takayama, S. Souma, T. Sato, T. Takahashi, Z. Wang, X. Dai, Z. Fang, G. F. Chen, J. L. Luo, and N. L. Wang, *Europhys. Lett.* **83**, 47001 (2008).
- [8] K. Terashima, Y. Sekiba, J. H. Bowen, K. Nakayama, T. Kawahara, T. Sato, P. Richard, Y.-M. Xu, L. J. Li, G. H. Cao, Z.-A. Xu, H. Ding and T. Takahashi, *Proc. Natl. Acad. Sci. U.S.A.* **106**, 7330 (2009).
- [9] Y. Zhang, L. X. Yang, F. Chen, B. Zhou, X. F. Wang, X. H. Chen, M. Arita, K. Shimada, H. Namatame, M. Taniguchi, J. P. Hu, B. P. Xie and D. L. Feng, *Phys. Rev. Lett.* **105**, 117003 (2010).
- [10] Y. Zhang, B. Zhou, F. Chen, J. Wei, M. Xu, L. X. Yang, C. Fang, W. F. Tsai, G. H. Cao, Z. A. Xu, M. Arita, H. Hayashi, J. Jiang, H. Iwasawa, C. H. Hong, K. Shimada, H. Namatame, M. Taniguchi, J. P. Hu, D. L. Feng, *Phys. Rev. B* (in press), preprint available as arXiv:0904.4022.
- [11] V. Vildosola, L. Pourovskii, R. Arita, S. Biermann, and A. Georges, *Phys. Rev. B* **78**, 064518 (2008); K. Kuroki, arXiv:1008.2286v1; R. Thomale et al., *Phys. Rev. B* **80**, 180505 (2009); R. Thomale, C. Platt, W. Hanke, and B. A. Bernevig, arXiv:1002.3599v1
- [12] T. Hanaguri, S. Niitaka, K. Kuroki, and H. Takagi, *Science* **23**, 441-443 (2010).
- [13] V-shaped scanning tunneling spectra has been observed in the superconducting state of α -FeSe by Q. K. Xue and co-workers (private communication).
- [14] J. K. Dong, S. Y. Zhou, T. Y. Guan, H. Zhang, Y. F. Dai, X. Qiu, X. F. Wang, Y. He, X. H. Chen, and S. Y. Li, *Phys. Rev. Lett.* **104**, 087005 (2010).
- [15] J. Guo, S. Jin, G. Wang, S. Wang, K. Zhu, T. Zhou, M. He, and X. Chen, *Phys. Rev. B* **82**, 180520 (2010).
- [16] Yoshikazu Mizuguchi, Hiroyuki Takeya, Yasuna Kawasaki, Toshinori Ozaki, Shunsuke Tsuda, Takahide Yamaguchi, and Yoshihiko Takano, arXiv:1012.4950 (unpublished).
- [17] A. Krzton-Maziopa, Z. Shermadini, E. Pomjakushina, V. Pomjakushin, M. Bendele, A. Amato, R. Khasanov, H. Luetkens, and K. Conder, arXiv:1012.3637 (unpublished).
- [18] J. J. Ying, X. F. Wang, X. G. Luo, A. F. Wang, M. Zhang, Y. J. Yan, Z. J. Xiang, R. H. Liu, P. Cheng, G. J. Ye, and X. H. Chen, arXiv:submit/0169761 (unpublished).
- [19] I. R. Shein, A. L. Ivanovskii, arXiv:1012.5164, (unpublished).
- [20] Fei Chen, Bo Zhou, Yan Zhang, Jia Wei, Hong-Wei Ou, Jia-Feng Zhao, Cheng He, Qing-Qin Ge, Masashi Arita, Kenya Shimada, Hirofumi Namatame, Masaki Taniguchi, Zhong-Yi Lu, Jiangping Hu, Xiao-Yu Cui, and D. L. Feng, *Phys. Rev. B* **81**, 014526 (2010).